Science of the Total Environment 890 (2023) 164215

Contents lists available at ScienceDirect

Science of the Total Environment

journal homepage: www.elsevier.com/locate/scitotenv

Toxicity of exhaust emissions from high aromatic and non-aromatic diesel fuels using *in vitro* ALI exposure system

Henri Hakkarainen [a,*], Anssi Järvinen [b], Teemu Lepistö [c], Laura Salo [c], Niina Kuittinen [c], Elmeri Laakkonen [c], Mo Yang [a], Maria-Viola Martikainen [a], Sanna Saarikoski [e], Minna Aurela [e], Luis Barreira [e], Kimmo Teinilä [e], Mika Ihalainen [d], Päivi Aakko-Saksa [b], Hilkka Timonen [e], Topi Rönkkö [c], Pasi Jalava [a]

[a] *Inhalation toxicology laboratory, Department of Environmental and Biological Sciences, University of Eastern Finland, P.O. Box 1627, 70211 Kuopio, Finland*
[b] *VTT Technical Research Centre of Finland, VTT, P.O. Box 1000, 02044 Espoo, Finland*
[c] *Aerosol Physics Laboratory, Physics Unit, Tampere University, P.O. Box 692, 33014 Tampere, Finland*
[d] *Fine particles and aerosol technology laboratory, Department of Environmental and Biological Sciences, University of Eastern Finland, P.O. Box 1627, 70211 Kuopio, Finland*
[e] *Atmospheric Composition Research, Finnish Meteorological Institute, P.O. Box 503, Helsinki 00101, Finland*

HIGHLIGHTS

- The toxicity of the exhaust from two diesel fuels with distinct aromatic contents were studied *in vitro* with ALI system.
- Results show that the higher aromatic content of diesel fuel increases exhaust emissions and their emissions.
- Genotoxicity was connected to the exhaust PM, whereas immunological responses were also evident with the gaseous phase.

GRAPHICAL ABSTRACT

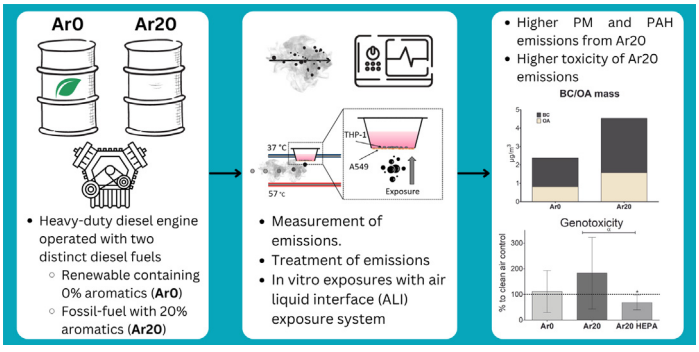

ARTICLE INFO

Editor: Pavlos Kassomenos

Keywords:
Engine exhaust
Air-liquid interface
Toxicity
Aromatic

ABSTRACT

The differences in the traffic fuels have been shown to affect exhaust emissions and their toxicity. Especially, the aromatic content of diesel fuel is an important factor considering the emissions, notably particulate matter (PM) concentrations. The ultra-fine particles (UFP, particles with a diameter of <100 nm) are important components of engine emissions and connected to various health effects, such as pulmonary and systematic inflammation, and cardiovascular disorders. Studying the toxicity of the UFPs and how different fuel options can be used for mitigating the emissions and toxicity is crucial. In the present study, emissions from a heavy-duty diesel engine were used to assess the exhaust emission toxicity with a thermophoresis-based *in vitro* air-liquid interface (ALI) exposure system. The aim of the study was to evaluate the toxicity of engine exhaust and the potential effect of 20 % aromatic fossil diesel and 0 % aromatic renewable diesel fuel on emission toxicity. The results of the present study show that the aromatic content of the fuel increases emission toxicity, which was seen as an increase in genotoxicity, distinct inflammatory responses, and alterations in the cell cycle. The increase in genotoxicity was most likely due to the PM phase of the exhaust, as the exposures with high-efficiency particulate absorbing (HEPA)-filtered exhaust resulted in a negligible increase in

Abbreviations: A549, Human Lung Type II Epithelial Cells; ALI, Air-Liquid Interface; BC, Black Carbon; CPC, Condensation Particle Counter; DDA, Differential Diffusion Analyser; DMEM, Dulbecco's Modified Eagle Medium; DR, Dilution Ratio; ELISA, Enzyme-Linked Immunosorbent Assay; ELPI, Electrical Low-Pressure Impactor; FBS, Fetal Bovine Serum; HEPA, High-Efficiency Particulate Absorbing; HEPES, 4-(2-Hydroxyethyl)-1-Piperazineethanesulfonic Acid; LDSA, Lung Deposited Surface Area; OA, Organic Aerosol; PAH, Polyaromatic Hydrocarbons; PM, Particulate Matter; PMA, Phorbol-12-Myristate-13-Acetate; SP-AMS, Soot Particle Aerosol Mass Spectrometer; SMPS, Scanning Mobility Particle Sizer; THP-1, Human Monocyte; UFP, Ultra-Fine Particles.

* Corresponding author at: University of Eastern Finland, Department of Environmental and Biological Sciences, P. O. Box 1627, FI-70211 Kuopio, Finland.
E-mail address: Henri.hakkarainen@uef.fi (H. Hakkarainen).

http://dx.doi.org/10.1016/j.scitotenv.2023.164215
Received 3 March 2023; Received in revised form 28 April 2023; Accepted 12 May 2023
Available online 23 May 2023

genotoxicity. However, the solely gaseous exposures still elicited immunological responses. Overall, the present study shows that decreasing the aromatic content of the fuels could be a significant measure in mitigating traffic exhaust toxicity.

1. Introduction

Global air pollution is one of the most important environmental risks threatening human health (Cohen et al., 2017; Forouzanfar et al., 2016), with the recent WHO 2021 report estimating an annual death toll of up to seven million. Exposure to ambient air pollution is associated with cardiopulmonary diseases, such as chronic obstructive pulmonary disease (COPD), diabetes, and neurodegenerative diseases, such as Alzheimer's diseases (Lim et al., 2010; Pearson et al., 2010; Forouzanfar et al., 2016; Maher et al., 2016; Cohen et al., 2017; Mazidi and Speakman, 2017). Therefore, decreasing air pollution levels is crucial. Thus, the need for several, technology-based solutions for decreasing emissions is emphasized (World Health Organization, 2021). Better after-treatment systems in combustion applications, cleaner fuels, cleaner energy production, and electric vehicles, are just a few of the possible solutions for lowering levels of air pollution (Sofia et al., 2020; Apicella et al., 2020). However, electrifying the heavy-duty fleet will be harder, as noted in the recent Euro 7 proposal, therefore, the need for cleaner combustion-based fuels in these applications will be relevant longer. (COM(2022) 586). Furthermore, research on combustion emissions and their effect on human health is essential. The increase in knowledge of the most harmful aspects of emissions will lead to more effective mitigation strategies.

Ultra-fine particles (UFP), particles with a diameter of <100 nm, are connected to various adverse health effects, such as pulmonary and systematic inflammation, and cardiovascular irregularities (Ohlwein et al., 2019). The surface-area to mass-ratio of UFPs is high, allowing UFPs to transport a high concentration of surface-bound components deep into biological systems (Kwon et al., 2020). Thus, UFPs have been speculated to be one of the most toxic components of ambient aerosols (Traboulsi et al., 2017). Notable about UFPs is that they can enter the blood circulation *via* the lungs, thus, affecting multiple organs of the body (HEI, 2013; Miller et al., 2017; Schraufnagel, 2020). Furthermore, UFPs can be translocated into cells with diffusion through lipid membranes, affecting cells that are generally not capable of phagocytosis (Geiser et al., 2005; Yacobi et al., 2010). The importance of UFPs to genotoxicity *in vitro* using an air-liquid interface (ALI) exposure system has been highlighted recently (Hakkarainen et al., 2022). The recent connections between neurodegenerative diseases and air pollution are linked to UFP exposure, as UFPs can penetrate the blood-brain barrier, in addition to direct transport to the brain *via* the olfactory bulb (Oberdörster et al., 2004; Calderón-Garcidueñas et al., 2015; Heusinkveld et al., 2016; Calderón-Garcidueñas et al., 2019). Moreover, a study by Park et al., 2020 suggested a pathological link, between UFP exposure and Alzheimer's disease *in vivo* due to redox imbalance in the hippocampus.

The importance of UFP monitoring was emphasized in the WHO 2021 report, as there is a lack of information due to missing standardization regarding the measurement of under 100 nm size fraction of PM. Indeed, ambient levels of UFP in the atmosphere have been staying constant in recent years (Presto et al., 2021). Moreover, the modern traffic after-treatment systems are not as effective with UFP emissions, compared to the PM with a larger size, and may actually increase the concentration of UFP within the exhaust emissions due to nucleation (Vaaraslahti et al., 2004; Kwon et al., 2020). Overall, research-based information on the levels and effects of UFPs should be improved, as stated in the WHO 2021 report, with one solution being to decrease the measured particle diameter cut-off to 10 nm from the 23 nm in the current vehicle exhaust emission legislation, with the addition of volatile particles to the measurement methodology (ICCT, 2019).

One of the major contributors to exhaust emissions is fuel. The composition of fuels has been shown to affect emissions and their toxicity (Jalava et al., 2012; Yang et al., 2018; Hakkarainen et al., 2020). For example, a higher ethanol contribution in fuel has been shown to decrease exhaust PM emissions and toxicity of emissions (Timonen et al., 2017; Hakkarainen et al., 2020). Moreover, the aromatic content of the fuels, referring to the concentration of unsaturated hydrocarbons with benzene-like structures, has a substantial role regarding emissions, especially PM concentration (Karavalakis et al., 2015). The aromatics work as a precursor of multiple toxic compounds of combustion emissions (Yang et al., 2019), and a reduction in aromatics has been connected to a decrease in emissions toxicity (Jalava et al., 2021; Karavalakis et al., 2015; Hakkarainen et al., 2020). Consequently, the concentration of aromatics is of high importance and has been aimed to be substituted with higher ethanol-gasoline blends for commercial gasoline fuels (EPA 2017). Fuels produced from non-fossil sources, such as renewable diesel, have been shown to have in addition of low aromatics, no sulphur, higher oxygen content, and higher cetane numbers than fossil fuels. These properties all increase engine performance and decrease emission toxicity (Wu et al., 2020). Moreover, the fuels produced from non-fossil sources have lower greenhouse gas emissions than fossil fuels (Jeswani et al., 2020).

In the present study, emissions from a modern high-speed heavy-duty diesel engine without aftertreatment were used to assess exhaust toxicity with a thermophoresis-based *in vitro* ALI exposure system (Ihalainen et al., 2019). The aim of the study was to evaluate the toxicity of engine exhaust UFPs from two distinct diesel fuels. A co-culture of the human adenocarcinomic alveolar epithelial cell line (A549) and human monocytic leukaemia cell line (THP-1) was used. The two diesel fuels were: fossil fuel with 20 % of aromatics (Ar20), and renewable diesel, with 0 % aromatic content (Ar0). To better understand the relative toxicity of different exhaust components, volatile material was removed from the particles in selected exposures. Additionally, the effect of gas-phase compounds on toxicity was tested by filtering the exhaust sample entering the ALI with high-efficiency particulate absorbing (HEPA) filter. Finally, to examine the effect of only the smallest PM size fraction, selected exposures were conducted using the differential diffusion analyser (DDA) classifies particles based on their diffusional movement. Several different toxicological endpoints were analysed from the cells after the one-hour exhaust exposure.

2. Materials and methods

2.1. Engine exhaust experiments

In the present study, the source for emissions was a high-speed heavy-duty (HD), non-road diesel engine, AGCO 44 AWIC (ACGO Power Oy, Finland), which was tested using an electric dynamometer developed in-house at VTT. Basic characteristics of the engine are found in supplementary materials S1 Table 1. The specifications of the dynamometer are also reported in the S1. The engine was a modern diesel engine equipped with a common-rail fuel injection system, which is less sensitive toward fuel properties such as density and viscosity, compared to the older engines equipped with a mechanical fuel injection system. Overall, the engine used in the experiments represents diesel engines applied to heavy-duty vehicles, non-road applications, and high-speed marine engines using distillate fuels. The engine was not equipped with any exhaust after-treatment system in the measurements.

The engine was operated by running two consecutive 1800 s long ISO 8178 ramped mode cycles (RMC-C1) to obtain a cycle that matches the standard 3600 s ALI sampling period. The RMC-C1 is a test cycle developed for non-road engines and it contains modes with different loads and engine speeds from idle to maximum power and linear transitions lasting 20 s

between the modes. Duration of one mode with constant speed and load varies from 126 to 248 s. The cycle is shown in the supplementary materials S1 Fig. 1.

2.1.1. Fuels

The following two fuels with different aromatic contents were used in the measurement campaigns with HD diesel engine: "Ar20" fuel meeting EN590 specification with 20 wt-% total aromatics representing conventional diesel and essentially aromatic-free "Ar0" fuel containing 0.1 wt-% total aromatics. Both test fuels are commercially sold. In addition to aromatic content, several other properties of fuels varied substantially, such as cetane number and polyaromatic hydrocarbon (PAH) content. Fuel properties were analysed by ASG Analytik-Service GmbH and can be seen in supplementary materials S1 Table 3.

2.1.2. Instrument setup

The instrument setup consisted of two different exhaust sampling systems, exhaust sample treatment systems, aerosol and gas instruments, and the ALI cell exposure system. The simplified overview of the measurement setup is shown in Fig. 1. Demonstration of the whole set-up is found in the supplementary materials S1 Fig. 2.

The exhaust was sampled from the tailpipe to several instruments including ALI by a porous tube diluter (PTD) combined with a residence time tube (RTT) together simulating the process of atmospheric dilution of the exhaust (Rönkkö et al., 2006; Keskinen and Rönkkö, 2010). A dilution rate (DR) of 12 was targeted within the PTD, and the dilution air temperature was maintained at 30 °C. After the RTT, a sample was led to an ejector diluter directly (DR 5) or through a thermodenuder. The direct option was used when particles containing semi-volatile compounds were studied and the thermodenuder option was used when non-volatile particles were studied. The thermodenuder, which removes volatile compounds from the particles, was operated at 265 °C.

After the ejector diluter, a sample was split between two lines: to the DDA-ALI system and to a set of real-time instruments.

The DDA was used to select the nano fraction (smaller than 10 nm) of the particles. When all the particles were studied, the classification was switched off. Downstream of the DDA additional clean air was added to the sample to reach a flow rate of 5 l/min required by the ALI, resulting in a DR of 6.67. A static mixer ensured a uniform sample to the ALI. The DDA classifies particles by their diffusion rates, allowing only particles smaller than 10 nm to pass through (Arffman et al., 2017). Particles below a certain size can be separated within the DDA by diffusion and guided to the ALI system for nanoparticle exposures. However, the device is still a prototype, with the present study being one of the first times it is used. The exposures which included the DDA are indicated by the term "Nano" within the exposure names. The effect of gaseous compounds was studied by removing particles from the sample with a HEPA-filter (HEPA Capsule 12144, Pall Corporation, Port Washington, NY, USA) in front of the ALI. These exposures are indicated by the term "HEPA".

Filter sampling of PM was conducted from the same line in parallel with the DDA. The sampling on quartz filters (Pallflex Tissuquartz, Pall Corporation, Port Washington, NY, USA) was performed with an eFilter (Dekati Ltd., Kangasala, Finland).

For most of the real-time instruments, the sample after the first ejector diluter was further diluted by two parallel ejector diluters (DR 5). A mixer and conical sampling tube were placed after the two ejector diluters to ensure proper mixing of the sample before being directed to the analysis instruments. The instruments in this sampling line included scanning mobility particle sizer (SMPS, TSI, inc., Shoreview, MN, USA, (Wang and Flagan, 1990) and Nano-SMPS, which were used to measure the particle number (PN) size distribution. PN concentration of particles larger than 10 nm was measured with a condensation particle counter (CPC A20, Airmodus Oy, Helsinki, Finland). An additional bridge diluter, followed by a mixer and flow splitter, was used upstream of the CPC to reduce particle concentration at the inlet in order to avoid exceeding the optimal concentration range of the instrument. An electrical low-pressure impactor (ELPI+, Dekati Ltd., Kangasala, Finland (Järvinen et al., 2014; Keskinen et al., 1992)) was utilized in the measurement of particle lung deposited surface area (LDSA) to compare possible differences of particle exposure between emissions of two distinct diesel fuels (Lepistö et al., 2022). LDSA is a metric that estimates the surface area of particles that enter the lung alveoli. Different compounds, for example, the total organic aerosol (OA) mass of PM were measured with a soot particle aerosol mass spectrometer (SP-AMS, Aerodyne Research Inc. Billerica, US, (Onasch et al., 2012)) and equivalent black carbon (eBC, hereon referred to as BC) concentration with an aethalometer (AE33, Magee Scientific, Slovenia, Drinovec et al., 2015)).

2.2. PAH

PAH concentrations were analysed from particles collected at the previous campaign, using the same fuels and engine. Concentrations are calculated using the percentage fractions of PAH from earlier campaign, therefore, concentrations of PAHs presented may not fully correspond to those which were in the aerosols of ALI exposures. The PAHs were analysed by a subcontractor, MetropoliLab, and a total of 24 individual PAH compounds (Supplementary materials S1 Table 6) were analysed according to ISO 16000 and EN 14662 analysis methods. The detection limits of the PAH analysis were 10–30 ng compound per sample and measurement uncertainty was 30 %.

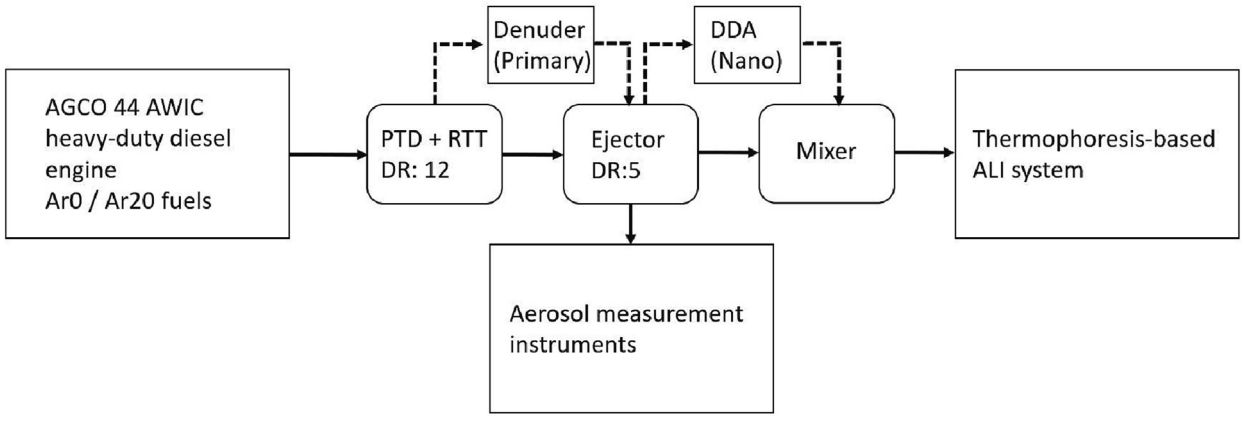

Fig. 1. Simplified overview of the instrumentation set-up. The exhaust sample was directed to the denuder for the Primary exposures and a differential diffusion analyser (DDA) was used with Nano exposures. The route of these experiments is marked with dashed arrows. Ar0 = Non-aromatic renewable diesel, Ar20 = 20 % aromatics fossil diesel, DR = Dilution Ratio, PTD = Porous Tube Diluter, RTT = Residence Time Tube, ALI = Air-Liquid Interface.

2.3. Exposures

The test matrix of this study is presented in Table 1. The highest priority and the largest number of repetitions were given to Ar20 fuel, as it represents the most used diesel fuel in Europe. Less commonly available aromatic-free Ar0 fuel and special sampling treatments received fewer repetitions. From both Ar20 and Ar0, three repetitions ($n = 3$) of the normal exhaust (also referred to as fresh) exposures were conducted. Additionally, one to three ($n = 1$–3), depending on the exposure, exposures with the DDA (denoted Nano) and exposures from which the volatile compounds were removed with thermodenuder (Primary), and a combination of both exposures (Nano Primary) were completed with both fuels. To examine the toxicity of gaseous exhaust compounds individually, from three Ar20 exhaust exposures (n = 3) particles were filtered out before the ALI using HEPA-filter. Moreover, as the concentrations of aerosols were higher in exposures without the DDA, to compare in more detail the absolute toxicity of only nanoparticle exposures, three exposures (n = 3) were conducted without DDA, but with similar concentrations as exposures including DDA (Reduced conc.). As the repetition count was low for the majority of the Primary and Nano exposures, with the addition of lacking aerosol data for Nano exposures, we have included in the figures results only from the Ar0, Ar20, and Ar20 HEPA exhaust exposures, whereas results from the Primary and Nano exposures are presented only in the table form. The clean air exposures were used as a control for the toxicological analyses and incubator controls as a control for the ALI exposure system ($n = 7$). The positive controls (n = 7) were lipopolysaccharide (LPS) for cytokine and methyl methanesulfonate (MMS) for genotoxicity analyses.

2.4. ALI exposure

The thermophoresis effect-based ALI *in vitro* exposure system was used to expose cells to different aerosols produced by the engine for 1 h. In this thermophoresis-based ALI exposure system, the aerosol exposure is conducted from the basal side of the inserts on to the A549 epithelium (Ihalainen et al., 2019). The main flow in the ALI was 5 l/min with a partial flow of 150 ml/min led to the cells as a laminar flow. The relative humidity of the ALI system approaches 100 %, while still staying below the condensation point at 37 °C. Deposition of particle mass, number, and surface area were calculated from the measured aerosol concentrations, similarly as in our previous studies using the same exposure system (Ihantola et al., 2020; Ihantola et al., 2022; Hakkarainen et al., 2022). The calculations are presented in supplementary materials S2 and the results in Table 4.

2.5. Cell culture

Co-culture of A549 human alveolar epithelial cells (ATCC®, CCL-158™) and THP-1 human monocyte cells (DSMZ ACC 16; German Collection of Micro-organisms and Cell Cultures; DSMZ, Germany) was cultured on 24 mm Falcon™ inserts (Corning, #353090, USA). The cells were cultured in a humidified incubator at +37 °C and 5 % CO_2 in Dulbecco's Modified Eagle (DMEM) supplemented with 10 % (v/v) fetal bovine serum (FBS), 2 mM L-glutamine, and 100 U/ml penicillin and 100 U/ml streptomycin (Sigma-Aldrich or Gibco, Life technologies).

The A549 cells were cultured on the basal side of the inserts' membrane four to six days preceding the exposures. The seeding densities of the cells depended on the exposure day and were 220 000 cells/ml, 200 000 cells/ml, and 180 000 cells/ml for inserts exposed four, five, and six days later, respectively. ALI environment was formed for A549 cells 48 h before exposure, by removing the cell medium and adding 1 ml of DMEM with 5 % of FBS only onto the apical side. THP-1 cells were differentiated 24 h before exposure, with 0.5 μg/ml phorbol-12-myristate-13-acetate (PMA) and seeded on the apical side of the inserts with the seeding density of 110 000 cells/ml. Thus, the percentage of THP-1s was approximately 10 % of the total cell count.

Prior to the exposure, the medium was replaced with serum-free medium supplemented with 25 mM 4-(2-hydroxyethyl)-1-piperazineethanesulfonic acid (HEPES) buffer (Sigma-Aldrich, USA), for buffering the alteration of pH. After the exposure, the medium was collected, and cells were supplied with a new serum-free medium and incubated for 24 h at +37 °C with 5 % CO_2. After the 24 h incubation, the medium was again collected from the inserts. Therefore, we can analyse the cytokine levels immediately (marked as 1 h) and 24 h (marked as 24 h) after the exposure.

Next, inserts were washed with phosphate-buffered saline (PBS) from both sides of the membrane. PBS was collected and trypsin-ethylenediaminetetraacetic acid (EDTA) solution was added to cells and incubated for 5 min at +37 °C with 5 % CO_2, detaching the cells from the inserts' membranes. To inhibit the trypsin, 100 μl of FBS was added, cells were rinsed from the insert membranes and collected in the same tubes as PBS earlier.

For analysis of genotoxicity, 60 μl of the cells were mixed with a freezing medium (50 % DMEM, 40 % FBS, and 10 % DMSO) and stored at −80 °C. For cell cycle analyses, a portion of the cells was pipetted in droplets to 4 ml of 70 % (v/v) ethanol under constant vortex-mixing and stored at +4 °C and analysed later.

2.6. Toxicological analysis

2.6.1. Genotoxicity

Genotoxicity was assessed with a slightly modified alkaline version of single-cell gel electrophoresis (SCGE), also known as comet assay. In the SCGE assay, the cells are embedded in agarose gel and lysed in alkaline settings, followed by electrophoresis. The lysing exposes the cell nucleoids, and the DNA supercoils with the alkaline conditions making DNA coils more relaxed, increasing the robustness of the assay. During the electrophoresis step, strand breaks in the DNA allow the negatively charged DNA to migrate more toward the positive anode of the electrophoresis chamber. The DNA strands can be stained with ethidium bromide and quantified with fluorescence microscopy. The level of genotoxicity is presented by the ratio of migrated DNA compared to unmigrated with data analysis done using the geometric median from the percentage of DNA in the tail. The detailed procedure for the SCGE assay is described in a previous study by Hakkarainen et al., 2022.

2.6.2. Cytokines

The immunological response of the cells was investigated by measuring the concentrations of the chemokine (C-X-C motif) ligand 1 (CXCL1), Tumor Necrosis Factor alfa (TNF-α), Interleukin 6 (IL-6), Interleukin 1 beta (IL-1β), Interferon gamma (IFN-γ), Interleukin 10 (IL-10), and Granulocyte-macrophage colony-stimulating factor (GM-CSF) from cell culture mediums. The secretion of CXCL1 was measured using an Enzyme-Linked Immunosorbent Assay (ELISA) kit (R&D Systems, Abington, UK) on 96-well plates (Nunc Maxisorp), according to the manufacturer's instructions. The measurements were conducted with a hybrid multi-mode reader Synergy H1 (BioTek Instruments, USA) at 450 nm.

Concentrations of GM-CSF, IFN-γ, IL-1β, IL-6, IL-10, and TNF-α were measured using U-PLEX Biomarker Group 1 (hu) 6-assay kit and Sector 2400 imager Reader (both from Meso Scale Diagnostics, USA) with

Table 1
Test point descriptions.

Test point	Fuel	Particle type	Size classification for ALI	Repetitions
1. Ar0	Ar0	Fresh	No	3
2. Ar20	Ar20	Fresh	No	4
3. Ar20 HEPA	Ar20	Gas phase only	HEPA filter	3
4. Ar0 Nano	Ar0	Fresh	Yes, nanoparticles with DDA	3
5. Ar0 Primary	Ar0	Primary	No	1
6. Ar0 Nano Primary	Ar0	Primary	Yes, nanoparticles with DDA	2
7. Ar20 Nano	Ar20	Fresh	Yes, nanoparticles with DDA	3
8. Ar20 Primary	Ar20	Primary	No	3
9. Ar20 Nano Primary	Ar20	Primary	Yes, nanoparticles with DDA	2
10. Ar20 Reduced conc.	Ar20	Fresh	No, reduced concentration	3

Discovery Workbench® 3.0.18 software. Analyses were conducted according to the manufacturer's instructions, using reagents provided with the kit. The detection limits (DL) were defined for each cytokine separately. Distributions of cytokines and detection ranges are shown in supplementary materials S1 Table 2. For samples where concentrations were below the lower DL, values corresponding to half of the DL (DL/2) of the respective cytokine assay were used.

Cytokines were measured from a medium collected directly after the exposure (referred to as 1 h) and after 24 h of incubation (24 h). The high percentage of levels of IFN-γ were below DL and thus excluded from the study. Moreover, the majority of the cytokines from the 1 h timepoint (except CXCL1 and IL-6) were not analysed due to the high percentage of concentrations below DLs. Data from cytokine measurements are shown as a percentage of difference compared to clean air control.

2.6.3. Cell cycle

In cell cycle assay, the RNA of the fixed and permeabilized cells is erased, followed by the staining of the DNA with propidium iodide (PI), a fluorescent agent which binds to the DNA through intercalation between the bases, and the analysed with FACSCanto II flow cytometer (BD Biosciences, USA). The stained DNA within the cells emits fluorescence signals proportional to the amount of cellular DNA. The RNA is first removed from the cells because PI binds to RNA as well, making the results impossible to interpret due to the fluorescence signal from RNA.

The cell suspensions fixed in ethanol were centrifuged, washed with 1 ml of cold PBS, and resuspended in 250 μl of cold PBS. 3.75 μl of RNAse A (10 mg/ml) was added to the samples and vortexed before a 1 h incubation at +50 °C. This was followed by adding 2.0 μl of PI (1 mg/ml), vortex-mixing, and 30 min incubation at +37 °C. The samples were measured with a FACSCanto II flow cytometer (BD Biosciences, USA). The data from measurements were analysed using FlowJo 10 software (FlowJo LLC, USA) and presented as cell population percentages in sub-G1/G0, G1/G0, and S + G2/M phases, compared to the respected clean air control levels. The G1 phase indicates cell growth, the S + G2_M cell mitosis, and the Sub_G1 phase indicates the state of apoptosis.

2.7. Statistical methods

Statistical analyses between groups were performed using Mann-Whitney *U* test. A *p*-value of <0.05 was considered to be statistically significant. Statistical analyses were performed using IBM SPSS Statistics for Windows, Version 27.0 (IBM Corp. Armonk, NY).

3. Results

3.1. Aerosol results

The different aerosol components and properties are presented in Table 2 in the diluted exhaust gas, preferring the aerosol concentrations which were led in the ALI system at exposures. Note that with all the exposures except for the Ar0, Ar0 Primary, Ar20, and Ar20 Primary, aerosol fed to the measurement devices was different from that the cells were exposed to in the ALI. Therefore, in the following tables, we only present properties (PM mass from the sum of OA and BC and from quartz filters, size with a geometric mean diameter (GMD), PN (> 10 nm), OA mass, BC mass, and masses of different OA families, as well as OA/BC -ratio) from the aerosols. The deposition estimates in the ALI system for PM mass, PN (> 10 nm), OA, and BC mass are shown in Table 3. The raw exhaust gas concentrations are presented in supplementary materials S1 Table 4. The PM mass from measurement instruments resulted in a bit higher concentration, compared to the filter samples. The Ar20 resulted in 88 % and 58 % higher PM mass concentrations in both fresh and Primary exposures, respectively. However, the OA and BC fractions were relatively similar in both fresh and Primary exposures, indicating that both OA and BC components increased in the same proportion when using Ar20. Based on the differences between primary and fresh emissions on average approximately only 20 % of OA stayed non-volatilized at 265 °C (Table 3). Regarding the composition of OA, OA consisted mostly of hydrocarbon fragments as the hydrocarbon fragment (C_xH_y) concentration was significantly higher than the one of oxygenated fragments (C_xH_yO and $C_xH_yO_z$) for all studied conditions. The main ion fragments were $C_4H_9^+$ and $C_3H_7^+$ from the alkyl chain (C_nH_{2n+1}) followed by $C_4H_7^+$ and $C_3H_5^+$ from the alkene chain (C_nH_{2n-1}). The high contribution of hydrocarbon-like OA is very typical for traffic-related exhaust emissions (Saarikoski et al., 2017). All mass spectra of the C_xH_y-family for both Fresh and Primary emissions as well as for both fuels (Ar0 and Ar20) were very similar (S3 Fig. 1) and do not explain the concentrations differences. It should be noted that fragmentation in AMS is the very strong and original structure of individual compounds can not be characterized. As the main difference between Ar20- and Ar0-fuels was the contribution of aromatics, the higher OA and BC concentrations when using Ar20-fuel were very likely connected to aromatic compounds. The contribution of particulate $C_6H_5^+$ ion which is a basic fragmentation ion from the aromatic ring was 0.9–3.2 % of the total hydrocarbon fragment. The contribution was higher for primary emissions than for fresh ones and for Ar20 than for Ar0 (S1 Fig. 3).

Fresh emissions in both fuels had relatively similar size distribution (mobility diameter) curve shapes, with Ar20 having a significantly higher number concentrations of particulates (Fig. 2). The concentration of UFPs in Primary exposures was multi-fold lower and the peak of particle size was in larger diameter particulates compared to fresh, resulting in an overall larger average PM size in Primary exposures.

BC and OA mass concentrations in the aerosols were higher from the Ar20 fuel, in both Primary and fresh emissions (Fig. 3). The organic fraction of the emissions from both fuels was multi-fold lower in primary aerosols. Note that organic mass concentrations were measured with a SP-AMS,

Table 3
Deposition estimates for PM mass, particle number (PN, > 10 nm), organic aerosol (OA) mass, and black carbon (BC) mass from four different exposures. PM mass is calculated from the sum of OA and BC. All values were calculated from concentrations in the diluted exhaust gas.

Test point	PM mass deposition (ng/cm^2)	PN deposition ($particles/mm^2$)	OA mass deposition (ng/cm^2)	BC mass deposition (ng/cm^2)
1. Ar0	2.1	7.3×10^4	0.7	1.4
2. Ar20	4.2	1.1×10^5	1.5	2.7
5. Ar0 Primary	1.1	1.0×10^4	0.2	0.9
8. Ar20 Primary	1.8	1.6×10^5	0.3	1.5

Table 2
PM mass as the sum of BC and OA and PM mass from quartz filters, geometric mean diameter (GMD), particle number (PN, > 10 nm), organic aerosol (OA) mass, black carbon (BC) mass, OA to BC mass percentage, and mean organics families' mass concentrations from four different exposures. Values are in the diluted exhaust gas, corresponding to concentrations led in the ALI system.

Test point	PM mass concentration ($\mu g/m^3$)	GMD (nm)	PN ($\#/cm^3$)	OA mass concentration ($\mu g/m^3$)	BC mass concentration ($\mu g/m^3$)	OA / BC	C_xH_y ($\mu g/m^3$)	C_xH_yO ($\mu g/m^3$)	$C_xH_yO_z$ (z > 1) ($\mu g/m^3$)
1. Ar0	2.4 / 2.6	15	8.1×10^4	0.8	1.6	0.5	0.70	0.06	0.04
2. Ar20	4.5 / 3.6	16	1.2×10^5	1.6	3.0	0.53	1.40	0.1	0.05
5. Ar0 Primary	1.2 / 1.3	32	1.1×10^4	0.2	1	0.2	0.13	0.04	0.03
8. Ar20 Primary	1.9 / -	32	1.8×10^4	0.2	1.7	0.12	0.16	0.03	0.02

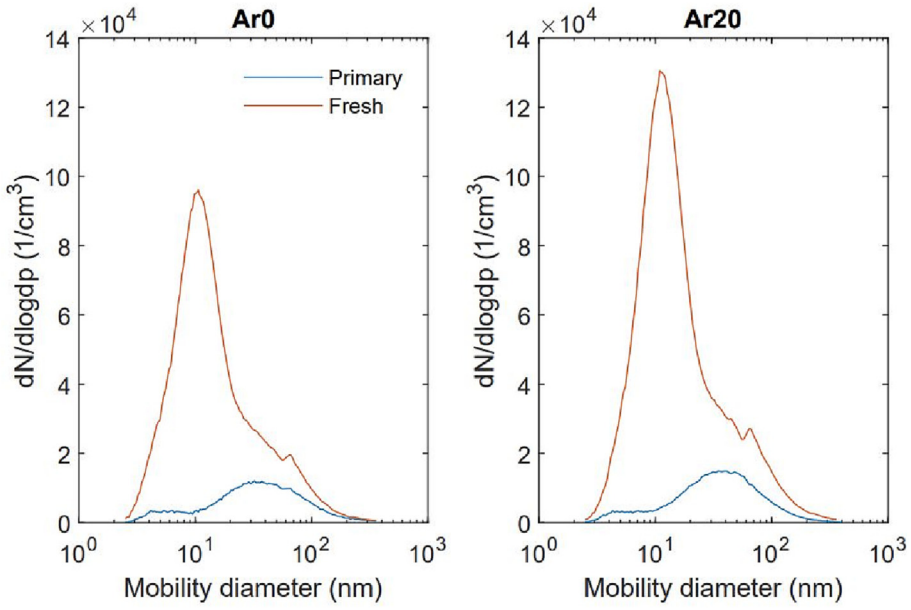

Fig. 2. Particle number size distribution (1/cm^3) for Ar0, Ar0 Primary, Ar20, and Ar20 primary exposures in the diluted exhaust gas. Fresh (normal) exposures are indicated by orange colour and Primary exposures with blue colour.

which includes only submicron particles with larger than 50 nm in aerodynamic diameter, and therefore, these results partly exclude the high PN concentrations which are seen in Fig. 2.

LDSA size distributions corresponding to the exhaust pipe concentrations of the two different fuel combustion are shown in Fig. 4. The results show that the higher particle emissions from Ar20 cause potentially more lung exposure than with Ar0 which could contribute to negative health effects. Also, Ar20 combustion contributes relatively more to lung deposition of particles smaller than 40 nm showing that also the characteristics and sizes of particles causing lung exposure are different, indicating varying health effects with the different fuels. In general, with both fuels, LDSA is mainly from soot particles smaller than 100 nm, which is typical for engine exhaust and near-traffic ambient aerosol (Lepistö et al., 2022).

3.1.1. PAH

The PM-bound PAH emissions from the diesel engine were considerably higher when using Ar20 as fuel (Fig. 5). Note that PAH analysis were not conducted during this experiment campaign, but the corresponding PAH concentrations were calculated using the PM masses between the campaigns. Raw exhaust gas concentrations of PAH compounds can be seen in supplementary materials S1 Fig. 4. This figure also includes the concentrations of PAH compounds in semi-volatile compound fraction. Based on

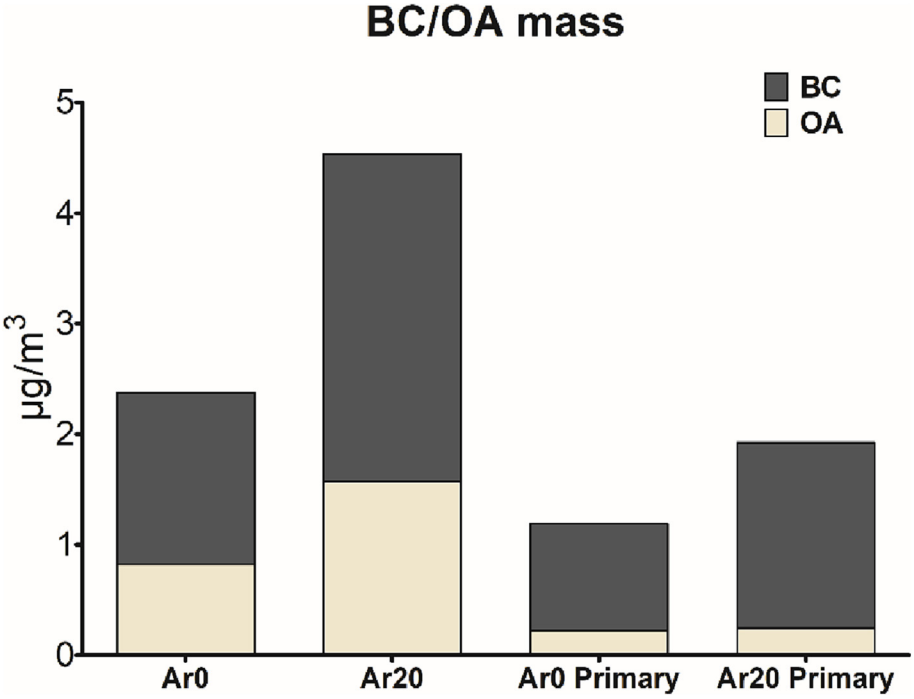

Fig. 3. Equivalent black carbon (BC) and organic aerosol (OA) mass concentrations (μg/m^3) from Ar0, Ar20, Ar0 Primary, and Ar20 Primary exposures in the diluted exhaust gas.

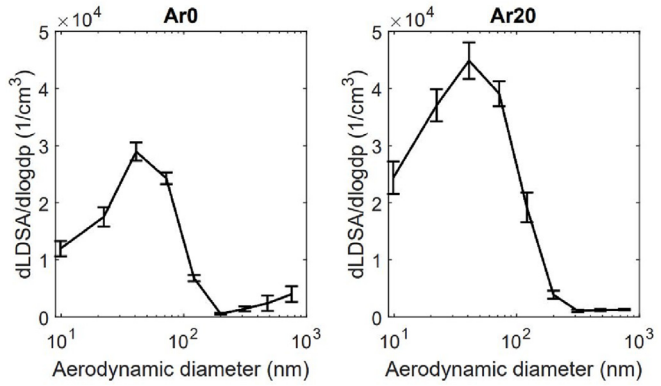

Fig. 4. Particle LDSA size distributions from Ar0 and Ar20 calculated from the exhaust pipe concentrations. The standard deviations of the distributions are indicated by vertical bars.

the fuel properties the PAH content in Ar20-fuel was 1.7 % and for Ar0 below 0.1 %. Of course, during the combustion of fuels, more PAH compounds might be formed. From the individual PAH compounds, pyrene was dominating species. The concentration of carcinogenic PAHs (presented as a line on the bar figures) was higher from the exhaust emissions of Ar20 fuel.

3.2. Toxicological results

The toxicological results of Ar0, Ar20, and Ar20 HEPA exposures are presented in the following figures. Results are compared to the clean air control with error bars showing a 95 % confidence interval (95 % CI) and the statistically significant differences (< 0.05 *p*-value) between the clean air control and different exposures are indicated with an asterisk and a line with alpha, respectively. Results from exposures that are not presented in the figure are shown in Table 4. In addition, all the exposures are presented in more detail in supplementary materials S1 Table 5. and the raw values are displayed in supplementary materials S3.

3.2.1. Genotoxicity

The highest genotoxicity was observed from the Ar20 exposure with an increase compared to the clean air control, whereas the Ar0 resulted in negligible difference (Fig. 6.). A statistically significant difference was found between the Ar20 and Ar20 HEPA exposures.

3.2.2. Cell cycle

Ar0 and Ar20 HEPA both resulted in similar levels of G1 cell cycle phase compared to clean air control (Fig. 7). Ar20 resulted in a statistically significant decrease in S + G2_M and an increase in G1 cell cycle phases compared to clean air control. A statistically significant difference was found between the Ar0 and Ar20 Sub_G1 cell cycle phases. Approximately 75 % of the cells are in the G1 phase, 22 % in the S + G2_M, and 3 % in the Sub_G1 cell cycle phases, respectively.

3.2.3. Cytokines

Exposure to all studied exhausts resulted in a statistically significant decrease in IL-1β and TNF-α levels in samples collected 24 h after the exposure when compared to control (Fig. 8). Exposure to Ar20 HEPA also lowered the levels of IL-10, CXCL1, and IL-6 and exposure to Ar20 lowered IL-6 secretion. In samples collected 1 h after the exposure, exposure to Ar20 and Ar20 HEPA resulted in higher levels of CXCL1.

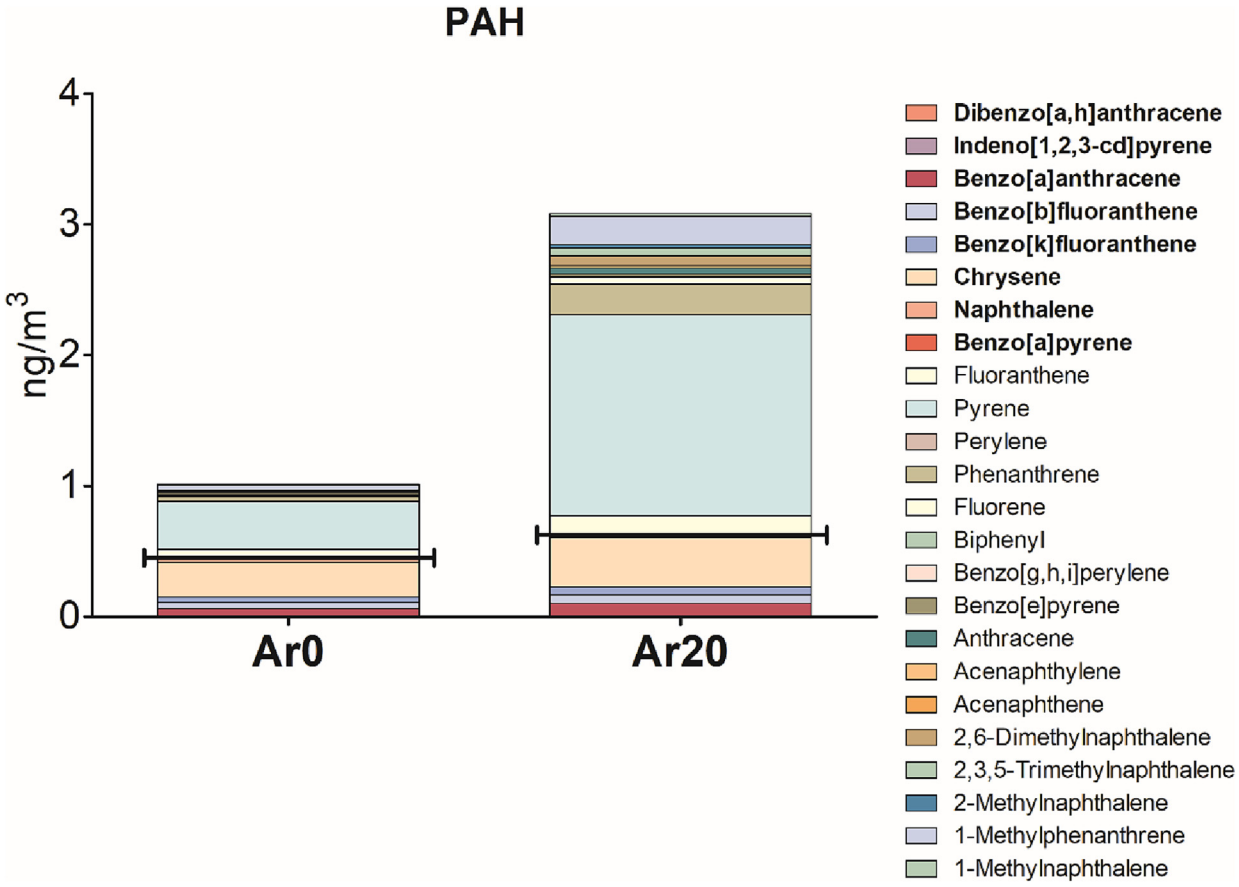

Fig. 5. Masses of PM-bound polyaromatic hydrocarbons measured in the diluted exhaust gas from two different fuels. Corresponding to concentrations within the ALI system. Carcinogenic PAHs are presented in bolded font and their sums with lines on the bar figures.

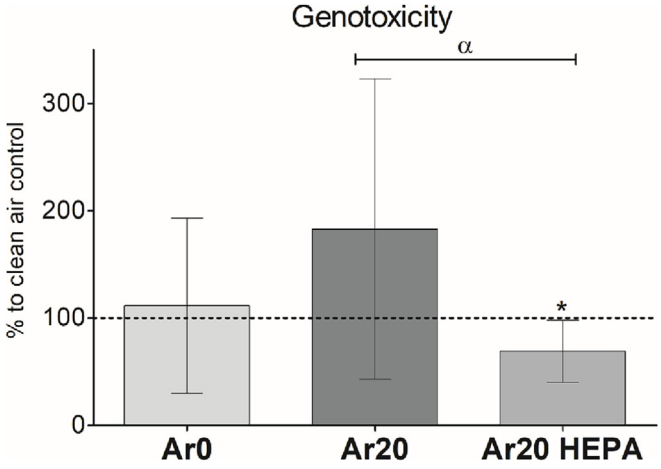

Fig. 6. Percent of genotoxicity after diesel exhaust exposures from A549 and THP-1 co-culture, compared to the clean air control with dashed line indicating the control. Results are shown as means with 95 % CI. $n = 3$. *p-value <0.05 compared to control and α = p-value <0.05 compared between different exposures.

When comparing exposures, a few differences were observed. The levels of IL-1β and CXCL1 differed statistically after Ar0 and Ar20 HEPA exposures (24 h samples). Interestingly, whilst all exposures elevated CXCL1 levels in samples collected after 1 h, the highest elevation was seen in Ar0, which differed significantly from both Ar20 and Ar20 HEPA.

Results from the exposures which are not shown in the figures are presented in supplementary materials S1 Table 5. Due to the low number of repetitions and lack of corresponding exposure aerosol data, it is not possible to fully draw conclusions about the toxicological effects between the results in Figs. 6 to 8.

The highest difference compared to clean air control with an increase in genotoxicity was seen in Ar20 Primary. However, no statistically significant results were seen in genotoxicity. The highest difference with a statistically significant increase in Sub_G1 cell cycle phases was observed with Ar20 Primary exposure. For the different cytokines, Ar20 Primary resulted in the highest difference with a statically significant increase between the clean air control in levels of GM-CSF, IL-1β, and TNF-α and with a statistically significant decrease in IL-10 and CXCL1. For IL-6, the highest difference with a statistically significant increase was with Ar20 Reduced conc. Exposure. Ar20 Nano and Ar0 Nano resulted in the highest difference compared to clean air control with statistically significant decrease and increase for 1 h

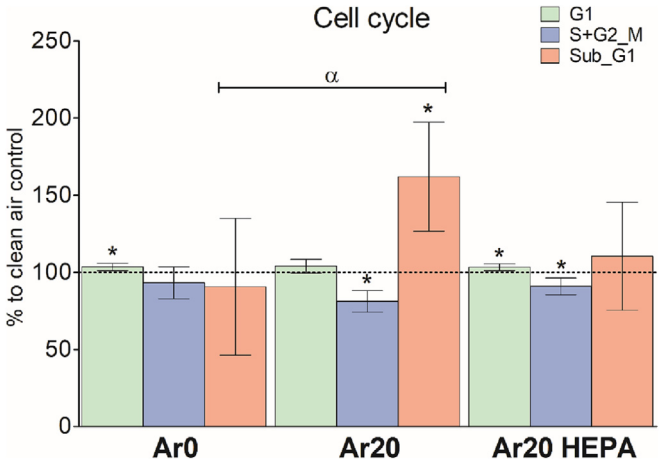

Fig. 7. Percent of different cell cycle phase populations after diesel exhaust exposures from A549 and THP-1 co-culture, compared clean air control with dashed line indicating the control. Results are shown as means with 95 % CI. $n = 3$. *p-value <0.05 compared to control and α = p-value <0.05 compared between different exposures.

levels of IL-6 and CXCL1, respectively. The lowest differences in toxicological endpoints were detected with Ar20 Reduced conc., with the least distinction compared to clean air control in genotoxicity and different cell cycle phases.

4. Discussion

In the present study, the emissions and emission toxicity of renewable diesel fuel (Ar0) differed when compared to those of fossil-based diesel (Ar20). Overall, PM mass and PN in the Ar20 fuel exhaust emissions were higher compared to the Ar0, whereas the particle size and OA/BC percentages between the different fuel exhausts were similar. As anticipated, the Ar0 fuel combustion also led to a lower concentration of PAH compounds, including the carcinogenic PAHs, similarly as in multiple previous studies comparing emissions of fossil- and renewable diesel fuels (Lu et al., 2012a, 2012b; Valle-Hernández et al., 2013; Steiner et al., 2013; Yilmaz and Donaldson, 2022). The results show the importance of the aromatic compounds in the fuel to the exhaust emissions. Also, the LDSA results follow the results with PN and mass concentrations, with over 75 % higher deposited surface area in the lung alveoli from the Ar20 emissions, demonstrating possible major differences with the health effects caused by the combustion of different fuels. Additionally, the LDSA results show that the average sizes of particles contributing to LDSA were slightly different, indicating that also the characteristics of particles entering the lung alveoli differ, which could lead to distinct health effects.

The exhaust emissions of two different fuels showed distinct toxicological effects. The overall mechanisms of PM-induced toxicity are complex due to the chemical complexity of the proxy and the biological complexity of the target and the interaction of those. The chemical composition of PM such as the concentration of metals and PAHs has been shown to affect health effects, due to their capability to produce oxidative stress and disturb normal homeostasis, leading to toxicological endpoints such as cytotoxicity, genotoxicity, and ultimately cell death (Shiraiwa et al., 2017; Riediker et al., 2019; Rönkkö et al., 2020). Furthermore, morphological aspects such as particulate size are important, affecting the ability of particulates to absorb and transport compounds to the deeper parts of the tissues and cells (Moreno-Ríos et al., 2022). The role of particles or particle-bound compounds as the culprits of genotoxicity is indicated in the present study by the Ar20 HEPA exposures, as the solely gaseous exposure did not increase genotoxicity. Mass concentrations of carcinogenic PAHs in semi-volatile compounds fraction and PM-bound fraction in Ar20 support this. However, in the earlier studies using wood combustion emissions with identical ALI system, the solely gaseous exposures resulted to increase in genotoxicity (Ihantola et al., 2020). Suggesting that the carcinogenic compounds in diesel exhaust are mainly bound to the particles, whereas, with wood combustion, the gaseous phase of the aerosol can be additionally genotoxic. Interesting is, however, why in the present study HEPA exposures resulted in lower genotoxicity compared to clean air control. A possible reason might be associated with cell cycle populations and a decrease of cell populations in the S-phase, as the cells in S-phase suffer more DNA damage due to the presence of replication processes (Kruszewski et al., 2012).

The Ar20 diesel exhaust induced higher genotoxicity compared to Ar0, which was seen in both Comet assay and the percentage of cells in the Sub_G1 phase of the cell cycle, as one of the major steps in apoptosis is DNA fragmentation. (Bai et al., 2017). Higher concentration of PM-bound PAH (especially the carcinogenic PAH) compounds in Ar20 emissions is one of the likely culprits of the higher genotoxicity *in vitro*, as they have been associated with genotoxicity in multiple different air pollution studies (Kamal et al., 2015; Billet et al., 2018; Kanashova et al., 2018; Ihantola et al., 2020; Ihantola et al., 2022). PAH genotoxicity is due to metabolic products of PAHs in biological systems, binding to DNA and forming so-called PAH-DNA adducts, disturbing the normal functionality of DNA, and resulting in genotoxicity (Ewa and Danuta, 2017). For example, in A549 cells, even the low concentrations of the benzo[*a*]pyrene (B[*a*]P) have been linked to the addition of PAH-DNA adducts and genotoxicity

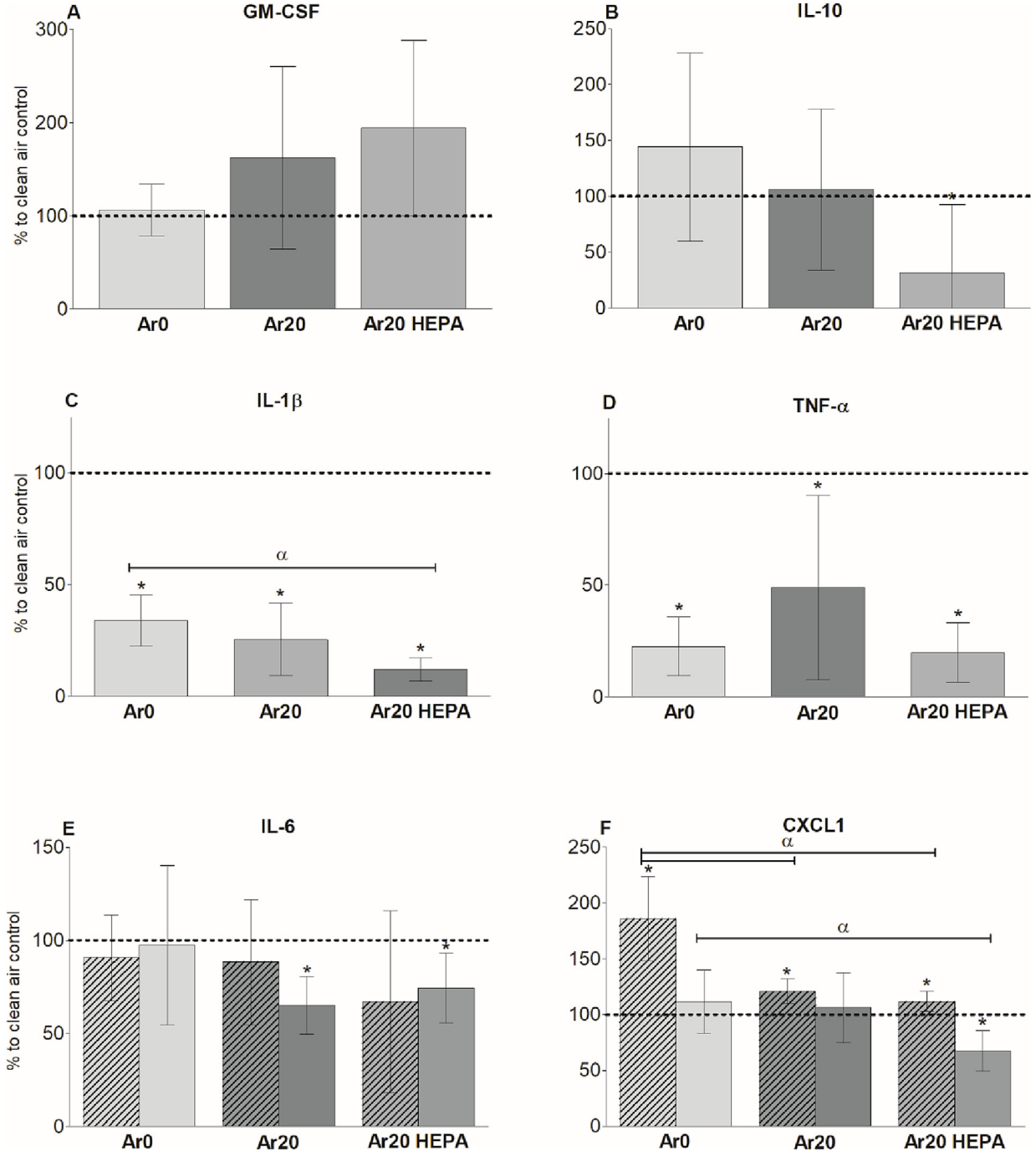

Fig. 8. Percent of different cytokine levels from A549 and THP-1 co-culture, compared to the control after exposure to diesel exhaust. A) GM-CSF, B) IL-10, C) IL-1B, D) TNF-a, E) IL-6, and F) CXCL1. All uniform bars present the 24 h samples and the bars with slash lines present the 1 h samples. Results are shown as means with 95 % CI. n = 3. *p-value <0.05 compared to control and α = p-value <0.05 compared between different exposures.

(Genies et al., 2013; Genies et al., 2016). Moreover, the UFPs can transfer the PAH compounds on their surfaces at high concentrations and within the intracellular space, thus, strengthening the toxicological effect of the PAHs (Moreno-Ríos et al., 2022). Additionally, the PAH compounds have been shown to localize in cytoplasm and result in toxicity *in vitro*, even when the particle localisation is on the extracellular side of the cell, as the PAHs can cross the lipid membrane due to their lipophilic character (Liu et al., 2021).

Another possible perpetrator for the genotoxicity is the particle size itself. It has been observed that the solid nanoparticles can yield genotoxicity without the PAH compounds, as seen in a study where mainly BC particles with an average diameter below 30 nm, resulted in high genotoxicity (Hakkarainen et al., 2022). Genotoxicity can rise from two different mechanisms which are called primary and secondary genotoxicity. In the primary, the DNA damage is induced by the particles with an absence of inflammation and the secondary includes the oxidative damage-inducing pathways resulting from the inflammation (Schins and Knaapen, 2007). The process of nano-sized particle induced primary genotoxicity is connected with the capability of particles to enter intracellular and even intranuclear parts of the cell, therefore, disturbing normal cell functions and inflicting toxicological responses (Perde-Schrepler et al., 2019). The mechanisms of genotoxicity due to nano-sized particles include alteration of cell metabolism, DNA lesions, mitochondrial damage, activation of inflammatory mediator synthesis, and generation of reactive oxygen species

(ROS) due to peroxidation of membrane lipids and/or release of radicals from the particle surfaces (Sukhanova et al., 2018). It has been shown that for the respiratory cells, particles with a diameter below 50 nm can enter the intracellular spaces (Ruenraroengsak et al., 2012), and since the average PM size in the present study with fresh exposures was below 20 nm, particulates were probably able to infiltrate the cell membranes and cause genotoxicity *via* the primary genotoxic route. Furthermore, results from Ar20 Primary exposure support that the genotoxicity was most likely due to the particle size, as the Ar20 Primary induced an increase in genotoxicity even with a low mass of OA. However, the chemical composition of PM between the two fuels still has importance. This is indicated by differences in genotoxicity between the fresh and Primary exposures from both fuels: Ar20 exposures resulted in high genotoxicity, whereas the Ar0 exposures did not. As the PM masses and sizes were similar in both Ar20 and Ar0 Primary exposures, the underlying reason for the high genotoxicity of Primary Ar20 is likely connected to the chemical composition of PM.

The decrease in cytokine levels has been associated with air pollution exposure *in vitro* and *in vivo* in previous studies (Happo et al., 2013; Martikainen et al., 2018). This decrease might be due to *e.g.* immunosuppression. Decreases in multiple identical cytokines due to diesel exhaust particle exposure have been suggested to be connected to the suppression of MyD88 pathways and activation of the NF-κB transcription factor (Sarkar et al., 2012). Overall, the cytokine results show a stronger immunological response from the Ar20 exposures, especially the Ar20 HEPA exposure, compared to the Ar0. The high decrease in cytokine levels after Ar20 HEPA exposure indicates that the gaseous fraction might play the biggest role in the immunosuppression seen after exposures. However, interestingly there were not so clear correlations between immunosuppression and genotoxicity, contrary to what was seen in the study of Hakkarainen et al., 2022. Moreover, the Ar20 Primary induced pro-inflammatory, while the Ar20 fresh exposures had immunosuppressive effects, indicating the immunotoxicological importance of the PM-bound OA compounds. Overall, cytokine results show that exposure to exhaust of diesel fuel with aromatics, induces a higher difference in multiple cytokine levels compared to the clean air control, similarly as observed in previous studies (Kooter et al., 2013; Malorni et al., 2017).

The concentration of PN emissions led through the DDA has been estimated to decrease to a maximum of 10 % from the initial concentration of a certain particle size range, compared to exposures without the DDA (Arffman et al., 2017). And as only sub 10 nm particles were included with DDA, the decrease in PM mass concentrations was considerably higher. The multi-fold lower PM concentrations of the Nano exposures were evident within the toxicological responses, as the Nano-exposures resulted in lower toxicity compared to the fresh and Primary exposures. Overall, it is difficult to state any conclusive results from the Nano exposures, as there were no aerosol data for the PM mass or average PM size from the Nano exposures. However, the exposure to Ar20 reduced concentration exhaust resulted in the least difference compared to clean air control in toxicity, therefore, slightly suggesting the higher toxicity of the only sub 10 nm particle exposures. Overall, the Nano exhaust exposures including DDA emphasize the need to conduct more toxicological and aerosol research including the very smallest particle sizes (Pedata et al., 2015; WHO 2021; Moreno-Ríos et al., 2022).

Overall, results reveal that the aromatic content of diesel fuel is an important aspect considering the toxic compounds of diesel exhaust emissions. The present study additionally emphasizes the role of UFPs as genotoxic drivers. Therefore, the chemical composition of diesel fuel can have an important role in the toxicity of the emissions, and eliminating the aromatics from the diesel fuel, with the addition of particle filters as after-treatment systems, can decrease the emission toxicity further. Even though the present study establishes similar results from the previous studies, the use of a novel ALI exposure system complemented with a thorough analysis of exhaust emissions, these results are crucial addition to the research field (Lu et al., 2012a, 2012b; Kooter et al., 2013; Steiner et al., 2013; Valle-Hernández et al., 2013; Malorni et al., 2017; Yilmaz and Donaldson, 2022).

5. Conclusions

In the present study, the effect of aromatic concentration of diesel fuel in emissions and their toxicity was studied using a thermophoresis-based ALI exposure system. Results indicate that the larger concentration of aromatics increased the PM and PAH exhaust emissions, which subsequently led to an increase in genotoxicity and immunological responses. The increase in genotoxicity was suggested to be induced by the particulate emissions, likely connected to the UFP size fraction. However, the exposure with only gaseous fraction also induced a decrease in cytokine levels, and therefore, the toxicity of the gaseous fraction of the emissions should not be ignored and requires further research. Overall, decreasing the aromatic content of diesel fuels using for example renewable diesel as in the present study could be substantial for mitigating the PM emissions from combustion-based emissions. Our future studies aim to reveal the effect of fuel on emissions toxicity with more detail, using passenger vehicles with several different fuels including modern after-treatment systems.

Supplementary data to this article can be found online at https://doi.org/10.1016/j.scitotenv.2023.164215.

CRediT authorship contribution statement

All authors contributed to writing the manuscript and approved the present version.

Performed experimental work: Henri Hakkarainen, Anssi Järvinen, Teemu Lepistö, Laura Salo, Niina Kuittinen, Elmeri Laakkonen, Mo Yang, Maria-Viola Martikainen, Sanna Saarikoski, Minna Aurela, Luis Barreira, Pasi Jalava.

Evaluated data: Henri Hakkarainen, Anssi Järvinen, Teemu Lepistö, Laura Salo, Niina Kuittinen, Elmeri Laakkonen, Mo Yang, Maria-Viola Martikainen, Sanna Saarikoski, Minna Aurela, Luis Barreira, Kimmo Teinilä, Mika Ihalainen, Hilkka Timonen, Topi Rönkkö, Päivi-Aakko-Saksa, Pasi Jalava.

Provided experimental and instrumental infrastructure: Hilkka Timonen, Topi Rönkkö, Päivi-Aakko-Saksa, Pasi Jalava.

Wrote and edited the manuscript: Henri Hakkarainen, Anssi Järvinen, Teemu Lepistö, Laura Salo, Niina Kuittinen, Elmeri Laakkonen, Mo Yang, Maria-Viola Martikainen, Sanna Saarikoski, Minna Aurela, Luis Barreira, Kimmo Teinilä, Mika Ihalainen, Hilkka Timonen, Topi Rönkkö, Päivi-Aakko-Saksa, Pasi Jalava.

Data availability

Data will be made available on request.

Declaration of competing interest

The authors declare that they have no known competing financial interests or personal relationships that could have appeared to influence the work reported in this paper.

Acknowledgements

Vaisala provided electrochemical gas sensors for this study and conducted an initial analysis of the gas data and Dekati provided one ELPI+ to be used in the measurements. We thank Hanne Vainikainen for her invaluable assistance with the Comet analysis.

Funding

Financial support from Black Carbon Footprint project funded by Business Finland (grant nr: 528/31/2019, 530/31/2019), participating companies, and municipal actors. Academy of Finland Flagship Programme "ACCC" (Grant numbers 337551, 337552) with the addition of University of Eastern Finland doctoral school EPHB funding, are gratefully acknowledged.

This project has received funding from the European Union's Horizon 2020 research and innovation programme under grant agreement No 814978 (TUBE).

References

Apicella, B., Mancaruso, E., Russo, C., Tregrossi, A., Oliano, M.M., Ciajolo, A., Vaglieco, B.M., 2020. Effect of after-treatment systems on particulate matter emissions in diesel engine exhaust. Exp. Thermal Fluid Sci. 116, 110107. https://doi.org/10.1016/j.expthermflusci.2020.110107.

Arffman, A., Juuti, P., Harra, J., Keskinen, J., 2017. Differential diffusion analyzer. Aerosol Sci. Technol. 51 (12), 1429–1437. https://doi.org/10.1080/02786826.2017.1367089.

Bai, H., Wu, M., Zhang, H., Tang, G., 2017. Chronic polycyclic aromatic hydrocarbon exposure causes DNA damage and genomic instability in lung epithelial cells. Oncotarget. 8 (45), 79034–79045. https://doi.org/10.18632/oncotarget.20891 (Published 2017 Sep 15).

Billet, S., Landkocz, Y., Martin, P.J., Verdin, A., Ledoux, F., Lepers, C., André, V., Cazier, F., Sichel, F., Shirali, P., Gosset, P., Courcot, D., 2018. Chemical characterization of fine and ultrafine PM, direct and indirect genotoxicity of PM and their organic extracts on pulmonary cells. J. Environ. Sci. 71, 168–178. https://doi.org/10.1016/j.jes.2018.04.022 (ISSN 1001-0742).

Calderón-Garcidueñas, L., Calderón-Garcidueñas, A., Torres-Jardón, R., Avila-Ramírez, J., Kulesza, R.J., Angiulli, A.D., 2015. Air pollution and your brain: what do you need to know right now. Prim. Health Care Res. Dev. 16, 329–345. https://doi.org/10.1017/s146342361400036x.

Calderón-Garcidueñas, L., Reynoso-Robles, R., González-Maciel, A., 2019. Combustion and friction-derived nanoparticles and industrial-sourced nanoparticles: the culprit of Alzheimer and Parkinson's diseases. Environ. Res. 176, 108574. https://doi.org/10.1016/j.envres.2019.108574.

Cohen, A.J., Brauer, M., Burnett, R., Anderson, H.R., Frostad, J., Estep, K., et al., 2017. Estimates and 25-year trends of the global burden of disease attributable to ambient air pollution: an analysis of data from the Global Burden of Diseases Study 2015. Lancet 389, 1907–1918. https://doi.org/10.1016/s0140-6736(17)30505-6.

COM(2022) 586 final. REGULATION OF THE EUROPEAN PARLIAMENT AND OF THE COUNCIL on type-approval of motor vehicles and engines and of systems, components and separate technical units intended for such vehicles, with respect to their emissions and battery durability (Euro 7) and repealing Regulations (EC) No 715/2007 and (EC) No 595/200.

Drinovec, L., Močnik, G., Zotter, P., Prévôt, A.S.H., Ruckstuhl, C., Coz, E., Rupakheti, M., Sciare, J., Müller, T., Wiedensohler, A., Hansen, A.D.A., 2015. The "dual-spot" Aethalometer: an improved measurement of aerosol black carbon with real-time loading compensation. Atmos. Meas. Tech. 8, 1965–1979. https://doi.org/10.5194/amt-8-1965-2015.

Ewa, B., Danuta, M.Š., 2017. Polycyclic aromatic hydrocarbons and PAH-related DNA adducts. J. Appl. Genet. 58 (3), 321–330. https://doi.org/10.1007/s13353-016-0380-3.

Forouzanfar, M.H., Afshin, A., Alexander, L.T., Anderson, H.R., Bhutta, Z.A., Biryukov, S., et al., 2016. Global, regional, and national comparative risk assessment of 79 behavioural, environmental and occupational, and metabolic risks or clusters of risks, 1990–2015: a systematic analysis for the Global Burden of Disease Study 2015. Lancet 388, 1659–1724. https://doi.org/10.1016/s0140-6736(16)31679-8.

Fuel Trends Report: Gasoline 2006– - 2016, 2017. Office of Transportation and Air Quality; U.S. Environmental Protection Agency; EPA-420-R-17-005; October. https://nepis.epa.gov/Exe/ZyPDF.cgi?Dockey=P100T5J6.pdf.

Geiser, M., Rothen-Rutishauser, B., Kapp, N., et al., 2005. Ultrafine particles cross cellular membranes by nonphagocytic mechanisms in lungs and in cultured cells. Environ. Health Perspect. 113 (11), 1555–1560. https://doi.org/10.1289/ehp.8006.

Genies, C., Maître, A., Lefèbvre, E., Jullien, A., Chopard-Lallier, M., et al., 2013. The extreme variety of genotoxic response to benzo[a]pyrene in three different human cell lines from three different organs. PLoS One 8 (11), e78356. https://doi.org/10.1371/journal.pone.0078356.

Genies, C., Jullien, A., Lefebvre, E., Revol, M., Maitre, A., Douki, T., 2016. Inhibition of the formation of benzo[a]pyrene adducts to DNA in A549 lung cells exposed to mixtures of polycyclic aromatic hydrocarbons. Toxicol. in Vitro 35, 1–10. https://doi.org/10.1016/j.tiv.2016.05.006.

Hakkarainen, H., Aakko-Saksa, P., Sainio, M., et al., 2020. Toxicological evaluation of exhaust emissions from light-duty vehicles using different fuel alternatives in sub-freezing conditions. Part. Fibre Toxicol. 17, 17. https://doi.org/10.1186/s12989-020-00348-0.

Hakkarainen, H., Salo, L., Mikkonen, S., Saarikoski, S., Aurela, M., Teinilä, K., Ihalainen, M., Martikainen, S., Marjanen, P., Lepistö, T., Kuittinen, N., Saarnio, K., Aakko-Saksa, P., Pfeiffer, T.V., Timonen, H., Rönkkö, T., Jalava, P.I., 2022. Black carbon toxicity dependence on particle coating: Measurements with a novel cell exposure method. Sci. Total Environ. 838 (4), 156543. https://doi.org/10.1016/j.scitotenv.2022.156543 (ISSN 0048-9697).

Happo, M.S., Uski, O., Jalava, P.I., Kelz, J., Brunner, T., Hakulinen, P., Mäki-Paakkanen, J., Kosma, V.M., Jokiniemi, J., Obernberger, I., Hirvonen, M.R., 2013. Pulmonary inflammation and tissue damage in the mouse lung after exposure to PM samples from biomass heating appliances of old and modern technologies. Sci. Total Environ. 443, 256–266. https://doi.org/10.1016/j.scitotenv.2012.11.004 (ISSN 0048-9697).

HEI, 2013. Understanding the Health Effects of Ambient Ultrafine Particles. HEI Perspectives 3. Health Effects Institute, Boston, MA.

Heusinkveld, H.J., Wahle, T., Campbell, A., Westerink, R.H.S., Tran, L., Johnston, H., Stone, V., Cassee, F.R., Schins, R.P.F., 2016. Neurodegenerative and neurological disorders by small inhaled particles. NeuroToxicology 56, 94–106 ISSN 0161-813X https://doi.org/10.1016/j.neuro.2016.07.007 ISSN 0161-813X.

ICCT, 2019. Recommendations For Post-euro 6 Standards For Light-duty Vehicles In The European Union. The International Council on Clean Transportation (ICCT).

Ihalainen, M., Jalava, P., Ihantola, T., Kasurinen, S., Uski, O., Sippula, O., Hartikainen, A., Tissari, J., Kuuspalo, K., Lähde, A., Hirvonen, M.-R., Jokiniemi, J., 2019. Design and validation of an air-liquid interface (ALI) exposure device based on thermophoresis. Aerosol Sci. Technol. 53 (2), 133–145. https://doi.org/10.1080/02786826.2018.1556775.

Ihantola, T., Di Bucchianico, S., Happo, M., et al., 2020. Influence of wood species on toxicity of log-wood stove combustion aerosols: a parallel animal and air-liquid interface cell exposure study on spruce and pine smoke. Part. Fibre Toxicol. 17, 27. https://doi.org/10.1186/s12989-020-00355-1.

Ihantola, T., Hirvonen, M.R., Mika, Ihalainen M., et al., 2022. Genotoxic and inflammatory effects of spruce and brown coal briquettes combustion aerosols on lung cells at the air-liquid interface. Sci. Total Environ. 806 (1), 150489. https://doi.org/10.1016/j.scitotenv.2021.150489 (ISSN 0048-9697).

Jalava, P.I., Aakko-Saksa, P., Murtonen, T., et al., 2012. Toxicological properties of emission particles from heavy duty engines powered by conventional and bio-based diesel fuels and compressed natural gas. Part. Fibre Toxicol. 9, 37. https://doi.org/10.1186/1743-8977-9-37.

Järvinen, A., Aitomaa, M., Rostedt, A., Keskinen, J., Yli-Ojanperä, J., 2014. Calibration of the new electrical low pressure impactor (ELPI+). J. Aerosol Sci. 69, 150–159. https://doi.org/10.1016/j.jaerosci.2013.12.006.

Jeswani, H.K., Chilver, A., Azapagic, A., Nov. 2020. Environmental sustainability of biofuels: a review. Proc. Math Phys. Eng. Sci. 476 (2243), 20200351. https://doi.org/10.1098/rspa.2020.0351.

Kamal, A., Cincinelli, A., Martellini, T., Malik, R., 2015. A review of PAH exposure from the combustion of biomass fuel and their less surveyed effect on the blood parameters. Environ. Sci. Pollut. Res. Int. 22, 4076–4098.

Kanashova, T., et al., 2018. Emissions from a modern log wood masonry heater and wood pellet boiler: composition and biological impact on air-liquid interface exposed human lung cancer cells. J. Mol. Clin. Med. 1.1, 23.

Karavalakis, G., Short, D., Vu, D., Russell, R., Hajbabaei, M., Asa-Awuku, A., Durbin, T.D., 2015. Evaluating the effects of aromatics content in gasoline on gaseous and particulate matter emissions from SI-PFI and SIDI vehicles. Environ. Sci. Technol. 49, 7021–7031. https://doi.org/10.1021/es5061726.

Keskinen, J., Rönkkö, T., 2010. Can real-world diesel exhaust particle size distribution be reproduced in the laboratory? A critical review. J. Air Waste Manage. Assoc. 60, 1245–1255.

Keskinen, J., Pietarinen, K., Lehtimäki, M., 1992. Electrical low pressure impactor. J. Aerosol Sci. 23 (4), 353–360.

Kooter, I.M., Alblas, M.J., Jedynska, A.D., Steenhof, M., Houtzager, M.M.G., van Ras, M., 2013. Alveolar epithelial cells (A549) exposed at the air–liquid interface to diesel exhaust: first study in TNO's powertrain test center. Toxicol. in Vitro 27 (8), 2342–2349. https://doi.org/10.1016/j.tiv.2013.10.007.

Kruszewski, M., Iwaneńko, T., Machaj, E.K., Ołdak, T., Wojewódzka, M., Kapka-Skrzypczak, L., Pojda, Z., 2012. Direct use of the comet assay to study cell cycle distribution and its application to study cell cycle-dependent DNA damage formation. Mutagenesis 27 (5), 551–558. https://doi.org/10.1093/mutage/ges018.

Kwon, H.S., Ryu, M.H., Carlsten, C., 2020. Ultrafine particles: unique physicochemical properties relevant to health and disease. Exp. Mol. Med. 52, 318–328. https://doi.org/10.1038/s12276-020-0405-1.

Lepistö, T., Kuuluvainen, H., Lintusaari, H., Kuittinen, N., Salo, L., Helin, A., Niemi, J.V., Manninen, H.E., Timonen, H., Jalava, P., Saarikoski, S., Rönkkö, T., 2022. Connection between lung deposited surface area (LDSA) and black carbon (BC) concentrations in road traffic and harbour environments. Atmos. Environ. 272. https://doi.org/10.1016/j.atmosenv.2021.118931.

Lim, S.S., et al., 2010. A comparative risk assessment of burden of disease and injury attributable to 67 risk factors and risk factor clusters in 21 regions, 1990–2010: a systematic analysis for the Global Burden of Disease Study. Lancet 380 (9859), 2224–2260.

Liu, X., Ma, J., Ji, R., Wang, S., Zhang, Q., Zhang, C., Liu, S., Chen, W., 2021. Biochar fine particles enhance uptake of Benzo(a)pyrene to macrophages and epithelial cells via different mechanisms. Environ. Sci. Technol. Lett. 8 (3), 218–223. https://doi.org/10.1021/acs.estlett.0c00900.

Lu, T., Huang, Z., Cheung, C.S., Jing, Ma J., 2012a. Size distribution of EC, OC and particle-phase PAHs emissions from a diesel engine fueled with three fuels. Sci. Total Environ. 438, 33–41 ISSN 0048-9697 https://doi.org/10.1016/j.scitotenv.2012.08.026.

Lu, T., Huang, Z., Cheung, C.S., Jing, Ma J., 2012b. Size distribution of EC, OC and particle-phase PAHs emissions from a diesel engine fueled with three fuels. Sci. Total Environ. 438, 33–41 ISSN 0048-9697 https://doi.org/10.1016/j.scitotenv.2012.08.026.

Maher, B.A., Ahmed, I.A., Karloukovski, V., MacLaren, D.A., Foulds, P.G., Allsop, D., Mann, D.M., Torres-Jardón, R., Calderon-Garciduenas, L., 2016. Magnetite pollution nanoparticles in the human brain. Proc. Natl. Acad. Sci. U. S. A. 113 (39), 10797–10801. https://doi.org/10.1073/pnas.1605941113 (Epub 2016 Sep 6. PMID: 27601646; PMCID: PMC5047173).

Malorni, L., Guida, V., Sirignano, M., Genovese, G., Petrarca, C., Pedata, P., 2017. Exposure to sub-10nm particles emitted from a biodiesel-fueled diesel engine: in vitro toxicity and inflammatory potential. Toxicol. Lett. 270, 51–61 ISSN 0378-4274 https://doi.org/10.1016/j.toxlet.2017.02.009 ISSN 0378-4274.

Martikainen, M.-V., Rönkkö, T.J., Schaub, B., et al., 2018. Integrating farm and air pollution studies in search for immunoregulatory mechanisms operating in protective and high-risk environments. Pediatr. Allergy Immunol. 29, 815–822. https://doi.org/10.1111/pai.12975.

Mazidi, M., Speakman, J., 2017. Ambient particulate air pollution (PM2.5) is associated with the ratio of type 2 diabetes to obesity. Sci. Rep. 7, 9144. https://doi.org/10.1038/s41598-017-08287-1.

Miller, M.R., Raftis, J.B., Langrish, J.P., et al., 2017. Inhaled nanoparticles accumulate at sites of vascular disease. ACS Nano 11 (5), 4542–4552.

Moreno-Ríos, A.L., Tejeda-Benítez, L.P., Bustillo-Lecompte, C.F., 2022. Sources, characteristics, toxicity, and control of ultrafine particles: an overview. Geosci. Front. 13 (1), 101147 ISSN 1674-9871 https://doi.org/10.1016/j.gsf.2021.101147 ISSN 1674-9871.

Oberdörster, G., Sharp, Z., Atudorei, V., Elder, A., Gelein, R., Kreyling, W., Cox, C., 2004. Translocation of inhaled ultrafine particles to the brain. Inhal. Toxicol. 16 (6–7), 437–445.

Ohlwein, S., Kappeler, R., Kutlar Joss, M., et al., 2019. Health effects of ultrafine particles: a systematic literature review update of epidemiological evidence. Int. J. Public Health 64, 547–559. https://doi.org/10.1007/s00038-019-01202-7.

Onasch, T.B., Trimborn, A., Fortner, E.C., Jayne, J.T., Kok, G.L., Williams, L.R., Davidovits, P., Worsnop, D.R., 2012. Soot particle aerosol mass spectrometer: development, validation, and initial application. Aerosol Sci. Technol. 46 (7), 804–817. https://doi.org/10.1080/02786826.2012.663948.

Park, J.P., Lee, J., Lee, S., Lim, S., Noh, J., Cho, S.Y., Ha, J., Kim, H., Kim, C., Park, S., Lee, D.Y., Kim, F., 2020. Exposure of ultrafine particulate matter causes glutathione redox imbalance in the hippocampus: a neurometabolic susceptibility to Alzheimer's pathology. Sci. Total Environ. 718, 137267. https://doi.org/10.1016/j.scitotenv.2020.137267 (ISSN 0048-9697).

Pearson, J.F., Bachireddy, C., Shyamprasad, S., Goldfine, A.B., Brownstein, J.S., 2010. Association between fine particulate matter and diabetes prevalence in the U.S. Diabetes Care 33 (10), 2196–2201. https://doi.org/10.2337/dc10-0698 (Epub 2010 Jul 13. PMID: 20628090; PMCID: PMC2945160).

Pedata, P., Stoeger, T., Zimmermann, R., et al., 2015. Are we forgetting the smallest, sub 10 nm combustion generated particles? Part. Fibre Toxicol. 12, 34. https://doi.org/10.1186/s12989-015-0107-3.

Perde-Schrepler, M., Florea, A., Brie, I., Virag, P., Fischer-Fodor, E., Vâlcan, A., Gurzău, E., Lisencu, C., Maniu, A.J., 2019. Size-dependent cytotoxicity and genotoxicity of silver nanoparticles in cochlear cells in vitro. Nanomater. 2019, 6090259. https://doi.org/10.1155/2019/6090259.

Presto, A.A., Saha, P.K., Robinson, A.L., 2021. Past, present, and future of ultrafine particle exposures in North America. Atmos. Environ. 10, 100109.

Riediker, M., Zink, D., Kreyling, W., et al., 2019. Particle toxicology and health - where are we? Part. Fibre Toxicol. 16, 19. https://doi.org/10.1186/s12989-019-0302-8.

Rönkkö, T., Virtanen, A., Vaaraslahti, K., Keskinen, J., Pirjola, L., Lappi, M., 2006. Effect of dilution conditions and driving parameters on nucleation mode particles in diesel exhaust: laboratory and on-road study. Atmos. Environ. 40, 2893–2901.

Rönkkö, T.J., Hirvonen, M.V., Happo, M.S., Ihantola, T., Hakkarainen, H., Martikainen, M.-V., Gu, C., Wang, Q., Jokiniemi, J., Komppula, M., Jalava, P.I., 2020. Inflammatory responses of urban air PM modulated by chemical composition and different air quality situations in Nanjing, China. Environ. Res. 110382 (ISSN 0013-9351).

Ruenraroengsak, P., Novak, P., Berhanu, D., Thorley, A.J., Valsami-Jones, E., Gorelik, J., Korchev, Y.E., Tetley, T.D., 2012. Respiratory epithelial cytotoxicity and membrane damage (holes) caused by amine-modified nanoparticles. Nanotoxicology. 6 (1), 94–108. https://doi.org/10.3109/17435390.2011.558643.

Saarikoski, S., Timonen, H., Carbone, S., Kuuluvainen, H., Niemi, J.V., Kousa, A., Rönkkö, T., Worsnop, D., Hillamo, R., Pirjola, L., 2017. Investigating the chemical species in submicron particles emitted by city buses. Aerosol Sci. Technol. 51 (3), 317–329. https://doi.org/10.1080/02786826.2016.1261992.

Sarkar, S., Song, Y., Sarkar, S., Kipen, H.M., Laumbach, R.J., Zhang, J., Strickland, P.A., Gardner, C.R., Schwander, S., 2012. Suppression of the NF-κB pathway by diesel exhaust particles impairs human antimycobacterial immunity. J. Immunol. 188 (6), 2778–2793. https://doi.org/10.4049/jimmunol.1101380.

Schins, R.P.F., Knaapen, A.M., 2007. Genotoxicity of poorly soluble particles Inhal. Toxicol. 19 (sup1), 189–198. https://doi.org/10.1080/08958370701496202.

Schraufnagel, D.E., 2020. The health effects of ultrafine particles. Exp. Mol. Med. 52, 311–317. https://doi.org/10.1038/s12276-020-0403-3.

Shiraiwa, M., Ueda, K., Pozzer, A., Lammel, G., Kampf, C.J., Fushimi, A., Enami, S., Arangio, A.M., Fröhlich-Nowoisky, J., Fujitani, Y., Furuyama, A., Lakey, P.S.J., Lelieveld, J., Lucas, K., Morino, Y., Pöschl, U., Takahama, S., Takami, A., Tong, H., Weber, B., Yoshino, A., Sato, K., 2017. Aerosol health effects from molecular to global scales. Environ. Sci. Technol. 51 (23), 13545–13567. https://doi.org/10.1021/acs.est.7b04417.

Sofia, D., Gioiella, F., Lotrecchiano, N., et al., 2020. Mitigation strategies for reducing air pollution. Environ. Sci. Pollut. Res. 27, 19226–19235. https://doi.org/10.1007/s11356-020-08647-x.

Steiner, S., Czerwinski, J., Comte, P., Popovicheva, O., Kireeva, E., Müller, L., Heeb, N., Mayer, A., Fink, A., Rothen-Rutishauser, B., 2013. Comparison of the toxicity of diesel exhaust produced by bio- and fossil diesel combustion in human lung cells in vitro. Atmos. Environ. 81, 380–388 ISSN 1352-2310 https://doi.org/10.1016/j.atmosenv.2013.08.059 ISSN 1352-2310.

Sukhanova, A., Bozrova, S., Sokolov, P., et al., 2018. Dependence of nanoparticle toxicity on their physical and chemical properties. Nanoscale Res. Lett. 13, 44. https://doi.org/10.1186/s11671-018-2457-x.

Timonen, H., Karjalainen, P., Saukko, E., Saarikoski, S., Aakko-Saksa, P., Simonen, P., Murtonen, T., Dal Maso, M., Kuuluvainen, H., Bloss, M., Ahlberg, E., Svenningsson, B., Pagels, J., Brune, W.H., Keskinen, J., Worsnop, D.R., Hillamo, R., Rönkkö, T., 2017. Influence of fuel ethanol content on primary emissions and secondary aerosol formation potential for a modern flex-fuel gasoline vehicle. Atmos. Chem. Phys. 17, 5311–5329. https://doi.org/10.5194/acp-17-5311-2017.

Traboulsi, H., Guerrina, N., Iu, M., Maysinger, D., Ariya, P., Baglole, C.J., 2017. Inhaled pollutants: the molecular scene behind respiratory and systemic diseases associated with ultrafine particulate matter. Int. J. Mol. Sci. 18 (2), 243. https://doi.org/10.3390/ijms18020243.

Vaaraslahti, K., Virtanen, A., Ristimäki, J., Keskinen, J., 2004. Nucleation mode formation in heady-duty diesel exhaust with and without a particulate filter. Environ. Sci. Technol. 38, 4884–4890. https://doi.org/10.1021/es0353255.

Valle-Hernández, B.L., Amador-Muñoz, O., Jazcilevich-Diamant, A., Hernández-López, A.E., Villalobos-Pietrini, R., González-Oropeza, R., 2013. Polycyclic aromatic hydrocarbons in particulate matter emitted by the combustion of diesel and biodiesel. Combust. Sci. Technol. 185 (3), 420–434. https://doi.org/10.1080/00102202.2012.726665.

Wang, S.C., Flagan, R.C., 1990. Scanning electrical mobility spectrometer. Aerosol Sci. Technol. 13 (2), 230–240. https://doi.org/10.1080/02786829008959441.

World Health Organization, 2021. WHO Global Air Quality Guidelines: Particulate Matter (PM2.5 and PM10), Ozone, Nitrogen Dioxide, Sulfur Dioxide and Carbon Monoxide. World Health Organization. https://apps.who.int/iris/handle/10665/345329 (License: CC BY-NC-SA 3.0 IGO).

Wu, G., Ge, J.C., Choi, N.J., 2020. A comprehensive review of the application characteristics of biodiesel blends in diesel engines. Appl. Sci. 10 (22), 8015. https://doi.org/10.3390/app10228015.

Yacobi, N.R., et al., 2010. Mechanisms of alveolar epithelial translocation of a defined population of nanoparticles. Am. J. Respir. Cell Mol. Biol. 42, 604–614.

Yang, J., Roth, P., Ruehl, C.R., Shafer, M.M., Antkiewicz, D.S., Durbin, T.D., Cocker, D., Asa-Awuku, A., Karavalakis, G., 2018. Physical, chemical, and toxicological characteristics of particulate emissions from current technology gasoline direct injection vehicles. Sci. Total Environ. 650, 1182–1194.

Yang, J., Roth, P., Durbin, T., Karavalakis, G., 2019. Impacts of gasoline aromatic and ethanol levels on the emissions from GDI vehicles: Part 1. Influence on regulated and gaseous toxic pollutants. Fuel 252, 799–811. https://doi.org/10.1016/j.fuel.2019.04.143 (ISSN 0016-2361).

Yilmaz, N., Donaldson, B., 2022. Combined effects of engine characteristics and fuel aromatic content on polycyclic aromatic hydrocarbons and toxicity. Energy Sources 44 (4), 9156–9171. https://doi.org/10.1080/15567036.2022.2129880.